

Photochemical & Photobiological Sciences

Accepted Manuscript



This is an *Accepted Manuscript*, which has been through the Royal Society of Chemistry peer review process and has been accepted for publication.

Accepted Manuscripts are published online shortly after acceptance, before technical editing, formatting and proof reading. Using this free service, authors can make their results available to the community, in citable form, before we publish the edited article. We will replace this *Accepted Manuscript* with the edited and formatted *Advance Article* as soon as it is available.

You can find more information about *Accepted Manuscripts* in the [Information for Authors](#).

Please note that technical editing may introduce minor changes to the text and/or graphics, which may alter content. The journal's standard [Terms & Conditions](#) and the [Ethical guidelines](#) still apply. In no event shall the Royal Society of Chemistry be held responsible for any errors or omissions in this *Accepted Manuscript* or any consequences arising from the use of any information it contains.

Journal Name

Photochemical & Photobiological Sciences

RSC Publishing

ARTICLE

Static magnetic field (SMF) sensing of the P_{723}/P_{689} photosynthetic complex

Cite this: DOI: 10.1039/x0xx00000x

AbhishekBhattacharya[†], MadhurimaChakraborty[†], Sufi O Raja, Avijit Ghosh, Maitrayee Dasgupta and Anjan Kr. Dasgupta*

Received 00th January 2012,
Accepted 00th January 2012

DOI: 10.1039/x0xx00000x

www.rsc.org/

ABSTRACT: Moderate intensity SMF are shown to act as a controller of the proteic potential in the coherent milieu of the thylakoid membranes. SMF of the order of 60-500mT induces memory like effect in photo-system I (PSI, P_{723}) emission with a correlated oscillation of photo-system II (PSII, P_{689}) fluorescence emission at 77K temperature. The observed magnetic perturbation effecting the thylakoid photon capture circuitry was also found to be associated with the bio-energetic machinery of the thylakoid membranes. At normal pH SMF causes an enhancement of PSI fluorescence emission intensity ($P_{723}/P_{689} > 1$), followed by a slow relaxation upon removal of SMF. Enhancement of the PSI fluorescence intensity also occurs under no-field condition if either the medium pH is lowered, or protonophores like carbonyl cyanide chlorophenylhydrazine or nigericin are added ($P_{723}/P_{689} \geq 2$). If SMF was applied at this low pH condition or in presence of protonophore, a reverse effect namely a reduction of the enhanced PSI emission was observed. As SMF is essentially equivalent to a spin perturbation, the observed effects can be explained in terms of spin re-organization, illustrating a memory effect at a bulk scale membrane re-alignment and assembly. The mimicry of conventional uncouplers by SMF is also notable, the essential difference being the reversibility and manoeuvrability of the latter (SMF). Lastly, the effect implies numerous possibility of externally regulating the photon capture in thylakoid membranes using controlled SMF.

Introduction

The role of static magnetic field in biological systems has been elusive for a long time^{1, 2}. SMF of moderate strength affects plants and photosynthetic bacteria³⁻⁵. SMF acts as a non-invasive electromagnetic stimulation for growth. Continuous 10mT SMF exposure maximized growth⁶ and increased the chlorophyll (chl.) concentration and photosynthetic rate of the cyanobacterium *Spirulina platensis*⁷. Similarly

magneto-sensing has been reported in plants^{8, 9} and in drosophila¹⁰. The only quantum mechanical description that may directly or indirectly explain these spin perturbation effect induced by SMF is the radical pair mechanism that emphasizes the role of triplet fusion¹¹. The specialized proteins e.g. cryptochromes⁹ play a role in that. Other than this, quantum coherence is reported in thylakoids¹². We must consider the fact that photosynthetic machinery constituting in the thylakoid

membranes of light harvesting organisms and higher plants have a dynamic spatio-temporal correlation in the localization of the photo-systems I and II i.e. PSI & PSII¹²⁻¹⁴. PSII localize in tubular stacks, grana and PSI localizes in stroma lamellae, grana margins and the grana-stroma interfacial regions¹⁵ constituting a single lumenal space¹⁶. It may be further noted that the photo-system I (PS I) is largely responsible for the regulation of ΔpH ^{17, 18}. Upon illumination, a coupling of linear electron flow from PSII to PSI with cyclic electron flow around PSI accomplishes photochemistry maintaining the H^+/e ratio at around 2¹⁹ within the chloroplast. The physiological output of this proton coupled cyclic electron flow around PSI being charge separation^{20, 21} and trans-thylakoid proton gradient establishment²² for efficient functioning of proteic kinetic barrier limited ATP-synthase (ATPase) complex²⁴. Protonophores act to dissipate this membrane potential barrier²⁵. Electron paramagnetic resonance studies of PSI^{26, 27} had indirectly implied probable influence of SMF on the cyclic electron flow around PSI²⁸⁻³⁰. PS I is one of two multi-subunit pigment-protein complexes embedded in the thylakoids of chloroplast and the inner membranes of cyanobacteria³¹. Eventually both PS I and PSII are known to constitute a number spin-state transitions and cross over occurring between iron selenium (Fe-S, Fe-Se) in PS I³² and Mn-clusters in PS II³³⁻³⁵. System as structured as the thylakoid is likely to be spin perturbed and re-align by SMF³⁶, such spins behaving as tiny magnets³⁷. The tiny magnets can emerge from unpaired spins of radicals³⁸ depending on their gyromagnetic ratio³⁹. However, SMF would lead to an energy change of the order of $-\mu\text{H}$, where μ is the magnetic moment of the resulting spin at a given thylakoid location and H is the

corresponding magnetic field. Classically it would be difficult to explain how kT (thermal energy) $\gg \mu\text{H}$, would act on the system. Such as for protons under 1T field, this energy is of the order of $1.76 \times 10^{-7}\text{eV}$, this being several orders of magnitude lower than thermal energy (0.04eV) at 300K.

In order to utilize this sophisticated machinery in a relevant manner with SMF acting as a non-invasive modulator, a detailed understanding of their interaction mechanism is necessary. The quantum effect is always realizable at the atomic or subatomic scale and at sub-zero temperature, but the point that needs to be addressed is how such an effect can have a bulk manifestation and that too in presence of large scale thermal fluctuations. To explain a plausible route of amplification of the quantum effect we have introduced a bio-energetic perspective and designed our experiments accordingly. AFM was used as an effective nano dimension tool for imaging membrane dynamics such as supramolecular arrangement, membrane diffusion, adhesion etc.^{40, 41} at an atomic resolution⁴². Thylakoid membranes were reported to undergo molecular crowding⁴³ with lateral and topographical diffusion and segregation⁴⁴. Morphological and topographical rearrangements of the membrane surface with pigment-protein complex remodelling were often associated with salt induced stacking and de-stacking of the grana components and stroma margins⁴⁵ and thylakoid membrane redistribution during state transition⁴⁶ were also reported. In essence, our observation suggests that this route may explain the bulk level manifestation of the spin perturbation and its retention even in absence of field. The similarity of SMF to a 'controllable uncoupler' is also highlighted.

Experimental section

Materials

Plant material

Arachis hypogaea plants were grown in a growth chamber at 25 °C with a 16 h photoperiod under 40 μmol of photons $\text{m}^{-2} \text{s}^{-1}$. Leaflets of an average diameter of 1 cm were collected from 3-4 week old plants.

Isolation of thylakoid membranes

Leaflets from *A. hypogaea* plants dark-adapted for 16 h, were used for thylakoid isolation⁴⁷. Isolation was done via intact chloroplast according to Bennett et al.⁴⁸ with minor modification. After homogenization, the homogenate was passed through a four layers of nylon cloth and then centrifuged at 300 g for 3 minutes to remove the debris. The supernatant was centrifuged at 4,000 g for 10 minutes to pellet down thylakoid membranes. The thylakoid membranes were washed twice with wash buffer after osmotic rupture and then were re-suspended in the storage buffer (0.1M sorbitol, 10 mM Tricine-NaOH (pH~ 7.8), 10 mM MgCl_2 , and 1 mM KCl). They were snap-cooled in liquid N_2 and stored at -80C. The preparations were protected from light and kept ice-cold during the isolation procedure. The thylakoid membrane suspension was then subjected SDS PAGE following the method described earlier⁴⁷. Figure 1a shows the SDS PAGE pattern in which the right panel shows the membrane fraction in which Lhc b1 and Lhc b2 are marked, the left panel representing the marker lane. Chlorophyll was extracted in 80% buffered acetone and determined according to Hipkins and Baker⁴⁹. All the reagents and effectors used were of analytical grade Sigma-Aldrich (USA) or SRL (India) products.

Methods

Low temperature Fluorescence emission spectroscopy (Hitachi 7000 Spectrofluorimeter, Japan) were conducted to measure the electron transition between PSII and PSI where the excitation light was provided from a Xenon light source. The excitation monochromator was set to 480nm (slit width of 5 nm). Emission was scanned from 650 to 800 nm (slit width of 10 nm). Dark adapted thylakoid membrane samples of 0.4 mg/ml Chlorophyll concentration were diluted in filtered (200 μm Millipore syringe filter) storage buffer

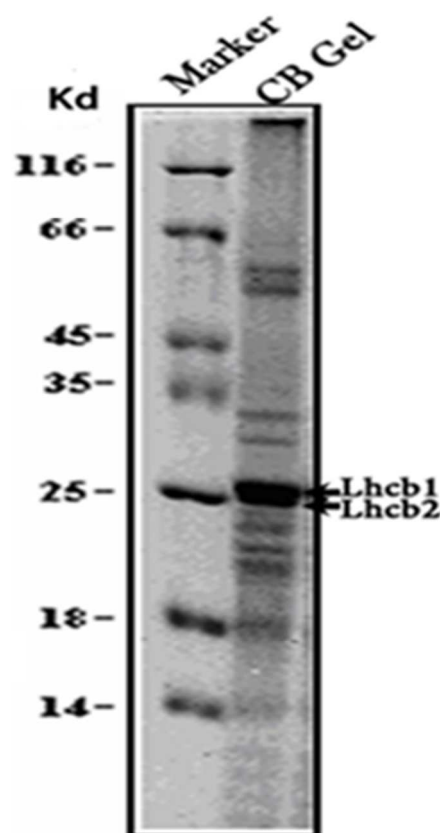


Fig. 1(a). SDS gel electrophoresis image of the thylakoid membrane fractions. The protein markers were run at the left panel whereas the right panel represents the membrane fractions. CB denotes to the comassie blue stained thylakoid membrane samples.

containing 70% glycerol (w/v), 20 mM HEPES buffer, pH 7.8, 5 mM MgCl₂, and 0.33 M sorbitol to a final concentration for fluorescence measurement of 10 μg ml⁻¹ chlorophyll.

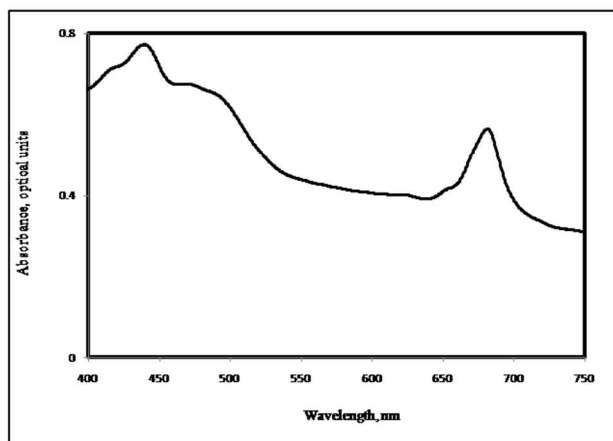


Fig.1(b). Absorbance spectra of the thylakoid membranes.

SMF exposure was imparted at 4°C for 10 minutes. Then the thylakoid membrane fractions were immediately frozen in liquid nitrogen in presence of appropriate cryoprotectant sorbitol. Data were also acquired at lower concentrations (4 μg ml⁻¹) of the membrane fractions to address any instance of self-absorption. Figure 1b shows the UV-Vis spectrum of the thylakoid suspension at room temperature, the spectrum being taken in a Agilent spectrophotometer (Model ,Carry 60 US). The spectra was taken at a wavelength interval of 0.5nm in the range of 400nm to 750nm.

To determine the SMF sensing behaviour of the thylakoid membranes, magnetic dose response study was performed by incubating the membranes at field strengths of 60, 120, 340 and 500mT. To determine the relaxation kinetics, SMF (500mT) incubation was initially performed for 10 minutes, and the field was then withdrawn. Following this magnetic incubation, measurement was made after zero-field incubation for 0,

5, 10, 20, 30 and 45 minutes respectively. All the experimental procedures and incubations were conducted at 4°C and at dark or dim light conditions. SMF effect on the membranes was also verified in presence of 10 μM DCMU, administered for 20 minutes. The bio-energetic perturbation study was performed by uncoupling the trans-membrane proteic status by different effectors which increase the proton permeability of the membranes and manipulate the proton potentials of these multipartite membranes. Firstly, the membrane proteic status was destabilized by lowering the pH at the outer membrane surface (stroma) with buffered 50mM L-ascorbic acid solution (pH 4) treatment for 5 minutes (targeting ΔΨ). Next, the samples were subjected to 6 μM Mnigericin (protonophore) treatment for 20 minutes for destabilization of the trans-membrane proton gradient (ΔpH). Also, the thylakoid membrane fractions were treated with 5 μM CCCP for 20 minutes. CCCP is an universal uncoupler of proton potential across the biological membranes. It acts as an ionophore and dissipates the ionic and hence proton potential gradient across the membrane (Δp). Protonophores effectively collapse the kinetic barrier of protons at the membrane surface effecting their access to the ATPase complex⁵⁰ in the PSI lamellae. At this state the membrane render non-functional bio-energetically. SMF exposure (500mT) at these bio-energetically destabilized conditions to the thylakoid membrane fractions and the magnetic sensing was acquired by low temperature spectroscopy and correlated to an altered diffusion behaviour measured using a dynamic light scattering set up (Malvern Nano ZS80, UK) equipped with a 532nm excitation laser source and a peltier system set at 4°C. Surface imaging of native biological membranes with atomic force

microscopy⁵¹ have the advantage of high resolution scanning at a sub-nano scale. The bulk scale topographical mapping of the photosynthetic membrane fractions was acquired with Nanoscope IVa (Veeco/Digital Instruments Innova, Santa Barbara, CA, USA) atomic force microscope (AFM). The measurements were made at the tapping mode in air. Soft silicon probes (RTESPA) were used with tip radius of 8 nm mounted on a single-beam cantilever (115-135 μ m). Cantilever deflections were recorded with a cantilever frequency (f_0) of 240- 308 KHz, horizontal scan rate of 1.2 Hz and 512 samples per line. The spring constant of the cantilevers was 20-80N/m. Imaging was performed at 25°C and the images were analysed by Nanoscope software (Version 5.12r3). 10-20 μ L of the control thylakoid membrane fractions (final concentration of 0.1 μ g/ml) and the SMF treated ones were immobilized on a modified hydrophilic glass cover chip allowing membranes to adhere to the surface. The remaining liquid was aspirated out and chips were air dried for microscopic study. The glass chips were pre-treated with piranha solution in heat bath for surface functionalization with hydroxyl group (-OH) on the glass surface, washed in chromic acid solution.

Results

Photosynthetic machinery constituting in spatially separated photo-systems (PSI and PSII) upon illumination undergo electronic transition. Cryogenic temperature data reveal the signature peak of PSII at 689nm⁵²(P₆₈₉) and a long wavelength emission maxima at 723nm originating from PSI³⁰(P₇₂₃). At dark adapted condition (closed photo centre) the ratio of the PSI/PSII fluorescence emission is close to 1 indicating that there was equal energy distribution between the two

oscillating photo-systems with respect to illumination (P₇₂₃/P₆₈₉ ~ 1). This ratio of P₇₂₃/P₆₈₉ emission is readily sensed by an external SMF source favouring down-hill energy transfer with P₇₂₃/P₆₈₉ > 1. This SMF induced spin dependent perturbation was shown to be directly translated into an altered photon capture profile of the photosynthetic components. Only 10 minutes of SMF (500mT) perturbation of the dark adapted thylakoid membrane fractions caused a 60.3% increase of PSI fluorescence intensity yield. This remarkable increase in PSI fluorescence intensity was correlated with a simultaneous decrease in the PSII fluorescence emission by 2.1%. Steady state (comparable to the dark control fluorescence emission values, P₇₂₃/P₆₈₉ ~ 1) was re-established only for cases where SMF was withdrawn several minutes (30-45 minutes) prior to measurement (Fig. 2a).

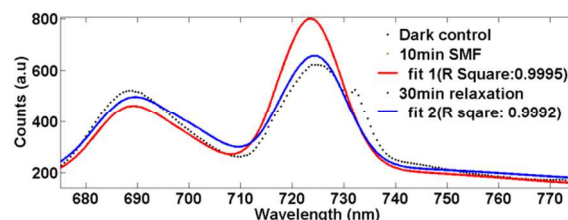


Fig. 2(a). SMF perturbation effect on thylakoid membrane fractions at low temperature. 77K spectra of dark control thylakoid membrane fractions (black dots), SMF treated (red) and 30 minutes post withdrawal membrane fractions undergoing relaxation (cyan) were represented. The plots were obtained by fitting the data to a best fit gauss model.

This SMF induced incremental alteration of PSI also holds true at lower concentrations of the membrane fractions denoting no instance of self-quenching behaviour.

This SMF induced spectral alteration was also replicated to a bulk scale shift in autocorrelation profile

of the thylakoid membranes reported in Fig. 2b. SMF perturbation resulted in a decrease in the number of scattering population (diffusion coefficient) denoting a distinct increase in the average hydrodynamic diameter (122nm to 295nm) and formation of intermediate species with almost 3 times shift in the autocorrelation delay times. This low spin perturbation effect was thus evident in the diffusion behaviour of the thylakoid membrane fractions. PSI/PSII (P_{723}/P_{689}) complex retains the memory of such weak perturbation.

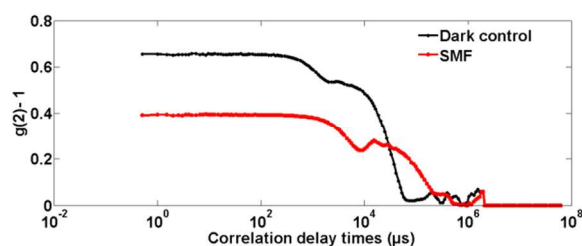


Fig. 2(b). Diffusion behaviour of the thylakoid membrane fractions illustrating an increment in size with a corresponding autocorrelation shift of the dark control (black) membrane fractions (122.4 nm) after SMF (red) perturbation (295.3 nm).

The photosynthetic machinery operates with a coupling between linear and cyclic electron flow for efficient capture of photon. This coupling can be perturbed by DCMU which is a blocker of electron transport between the two photo-systems (PSII and PSI). DCMU blocks electron transport between Quinone (Q_A to Q_B) cycles. Hence, linear electron transport from PSII to PSI was ceased. Although, cyclic electron flow along the PSI can be redundant. It can also be inferred from the DCMU data that at closed photo-centre (PC) conditions (dark adapted membrane fractions) there was no evidence of spill-over between the two photo-systems [S1].

The thylakoid membrane fractions were readily sensed by SMF with an exponentially related increase in $\Delta(\text{PSI/PSII})$ profile with varying field strengths (Fig. 3). This increment of PSI/PSII was cooperative depending on the time of exposure to the field strength (Table 1). Continuous SMF exposure for only 10 minutes resulted sufficient for spin re-organization.

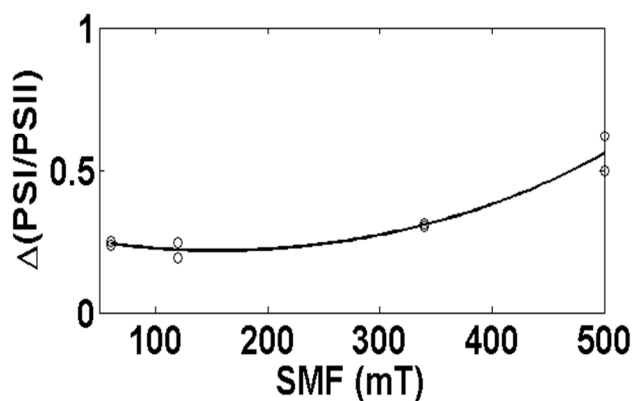


Fig. 3. Dose (magnetic field) response of the thylakoid membrane fractions: Ordinate and abscissa represents the incremental change in $\Delta(\text{PSI/PSII})$ ratio and SMF strength (mili-Tesla) respectively. The data were fitted to a best fit model: $(x) = a*\exp(b*x) + c*\exp(d*x)$.

Table 1. SMF exposure time (minutes) influence on the thylakoid membrane fractions. STD denotes standard deviation of each replicated data.

TIME OF INCUBATION (minutes)	PSI/PSII	STD (+/-)
0	1.041	0.050
2	1.24	0.077
4	1.37	0.021
6	1.46	0.007
10	2.141	0.084
20	1.585	0.104
30	1.52	0.033
45	1.516	0.094

This spin dependent re-organization of the membrane fractions showed relaxation upon removal of the external SMF source (Fig. 4). The magnetic relaxation kinetics was fitted to a dual time scale exponential decay expressed by:

$$\frac{dx}{dt} = 0.21 e^{-x/T1} + 1.64 e^{-x/T2} \dots(1)$$

Where, x represents the change in the PSI/PSII, the fitted values of T1 was 12.66 (min) and 1428 (min) for T2 (Fig. 3). Large T2, indicates lesser decay (or constant zero order change) in the relaxation, while the relatively faster decay is represented by the 12 min relaxation. At time \gg the T1 (say, 45 min) the PSI/PSII ratio enhancement approximately reverts back to dark control values. T1 value is of the order of spin lattice relaxation that originates from interaction of spin with local magnetic environment bearing π -ring containing macro cyclic pigment molecule chlorophyll. T2 may originate from the interaction of SMF induced spins with the ferromagnetic centres inside photo-systems.

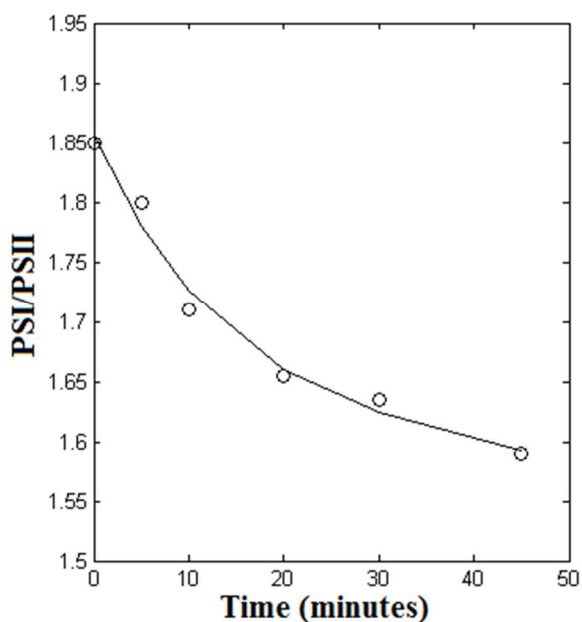


Fig. 4. Relaxation kinetics of SMF perturbed photo-system. The PSI/PSII ratio plot with time function (minutes) at the X-axis.

The higher values of T2 (compared to T1) may be correlated with long-term changes in the thylakoid membrane, e.g. its diffusional behaviour (Fig. 2b, 5b, 6b, 7b) and topographical re-organization (Fig. 9-11).

The circulatory coupled electron-proton flow is one of the other primary targets of SMF. SMF manifested dynamic spin dependent modulation of bio-energetically destabilized membrane fractions by different effectors. The samples were subjected to an osmotic shock with buffered L-ascorbic acid (pH4.0). L-ascorbic acid (L-Asc) is a natural antioxidant and monodehydroascorbate, a derivative of L-Asc is an electron acceptor at the reducing side of PSI⁵³. At dark adapted condition the stromal pH of the thylakoid membrane is about 7.8. Lowering of the pH of the buffered medium at the stromal side of the membrane fractions cause an inversion of the $\Delta\Psi$ component of the Δp resulting in an enhancement of PSI($P_{723}/P_{689} > 2$). Surprisingly, this phenomenon was reversed upon exposure to SMF comparable to the dark control fluorescence emission values ($P_{723}/P_{689} = 1$) (Fig. 5a). Although, L-Asc treated thylakoid membrane fractions showed minimal

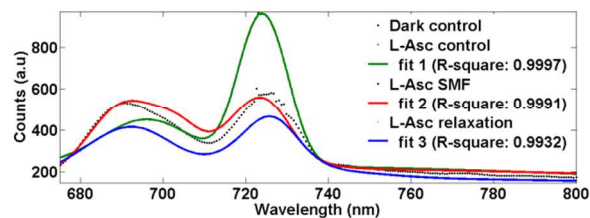


Fig. 5(a). Low temperature (77K) spectra of dark control thylakoid membrane fractions (black dots), buffered 50mM L-ascorbic acid treated membrane fractions (green), SMF perturbed L-ascorbic acid treated membranes (red), and 30

minutes post withdrawal relaxation profile (cyan) of the membrane fractions. The plotted data were fitted to the best fit gauss model.

alteration in the autocorrelation profile with SMF (Fig. 5b) depicting least discrepancy in the diffusional slope. A minimal increment in the average hydrodynamic diameter (size) was observed after SMF treatment at this L-Asc treated condition.

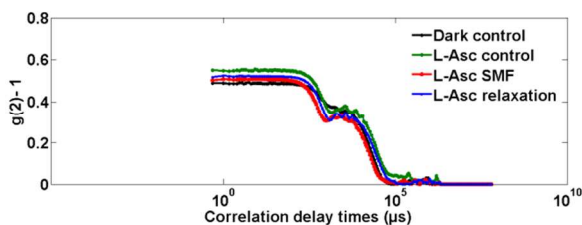


Fig. 5(b). Autocorrelation profile of $\Delta\Psi$ inverted membrane fractions; a minimal change in the size and autocorrelation was evidenced with respect to the dark control thylakoid (black) membrane fractions (122.4 nm), L-ascorbic acid (green, size of 141.8 nm) and SMF effect on L-ascorbic acid treated thylakoid (red) membrane fractions (141.8 nm) and relaxation (cyan).

Increase in membrane proton permeability by nigericin (targeting the ΔpH component of the Δp), also enhanced PSI/PSII fluorescence ratio. This PSI fluorescence enhancement too was reversed by SMF as compared to dark control values (Fig. 6a).

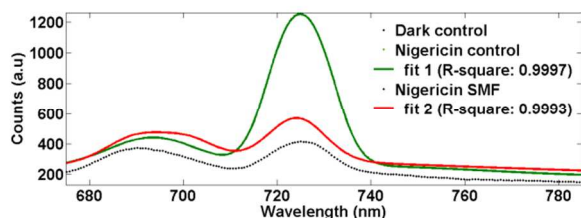


Fig. 6(a). ΔpH destabilization effect on the membrane fluorescence emission profile at 77K. Dark control thylakoid

membrane fractions (black dots), protonophore nigericin treated membrane fractions (green) and SMF perturbed membrane fractions at the destabilized condition (red) were represented. The data were fitted to a best fit gauss model.

This change in spectral profile was also reflected in the autocorrelation shift of almost 2.7 and intermediate species formation upon SMF induced spin perturbation at this bio-energetically destabilized condition (Fig. 6b).

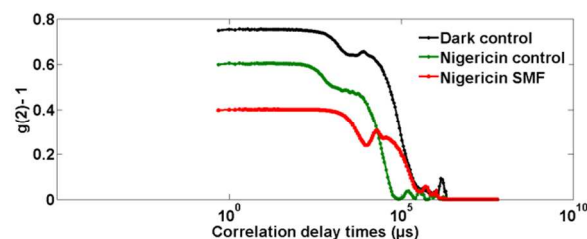


Fig. 6(b). Represents diffusional alteration of the ΔpH destabilized membrane fractions with protonophore nigericin. A huge increase in size with respect to the dark control (black) thylakoid membrane (122.4 nm), and nigericin (green, 122.4 nm) was evidenced upon SMF perturbation on the nigericin treated (red) thylakoid membranes (342 nm).

A decrease in the diffusion coefficient of the membrane fractions after SMF exposure with respect to the control and bio-energetically destabilized state implies increase in average hydrodynamic diameter of thylakoids (increasing from 122nm to 342nm). The deviation from spherical shape however makes this estimate approximate, but the robust trend nevertheless holds true. The fact is supported by an increase in scattering population (zero time intercept) and by the decrease in slope of the log linear portion of the autocorrelation decay profile. Again, the trans-thylakoid Δp itself was dissipated with CCCP administration. At this bio-energetically inert state the PSI/PSII ratio also increased

drastically. SMF perturbation at this state ($\Delta p \sim 0$) also tend to reverse the PSI/PSII ratio to a substantial amount, although not completely to the dark adapted fluorescence values (Fig. 7a). Hence, the membrane fractions at the vicinity of SMF always have a tendency to conserve its functional state (bio-energetic steady state) at the dark while SMF acting as a non-invasive uncoupler resistant probe.

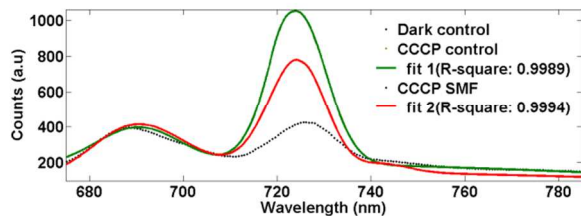


Fig. 7(a). Δp destabilizing effect on membrane 77K emission profiles. Dark control thylakoid membrane fractions (black dots), CCCP treated Δp destabilized membrane fractions (green); SMF perturbed Δp destabilized membrane fractions (red). All the data were fitted to a best fit gauss model.

This uncoupling effect was also realized at the diffusion behaviour of the membranes (Fig. 7b). Although there was a little change in the number of scattering population and subsequent hydrodynamic diameter after SMF treatment accompanied by a minor shift in the correlation delay timescales and the slope.

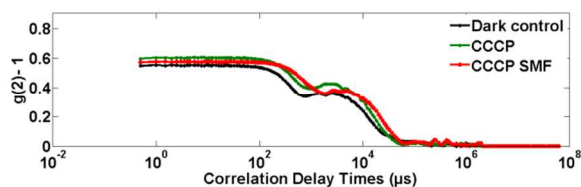


Fig. 7(b). Diffusion behaviour of the Δp destabilized membrane fractions with CCCP. A minor decrease in the hydrodynamic diameter of the membrane fractions were observed with respect to the dark control (black) thylakoid

membrane (175.8 nm), and CCCP (green, 92.65 nm). A marginal increase in size was observed upon SMF perturbation on the CCCP treated (red) thylakoid membranes (122.4 nm).

Upon SMF perturbation on the dark control thylakoid membrane fractions ($P_{723}/P_{689} = 1$), a distinct increment in the PSI with a minimal change in PSII profile was evident ($P_{723}/P_{689} > 1$). Whereas, bio-energetically ($\Delta \Psi$, ΔpH and Δp) destabilized membrane fractions itself revealed an increased PSI ($P_{723}/P_{689} > 2$) which upon SMF perturbation quenched back to the dark control fluorescence emission values ($P_{723}/P_{689} \sim 1$). The correlated change in the emission profiles of the photosynthetic components (PSI and PSII) was evident from the histogram bar graph [S2]. All the experimental data were verified statistically with coefficients having 95% confidence bound and fitted to a best fit model (using MATLAB R2013b software).

This unique and differential sensitivity of the photosynthetic components to SMF is indicative of both alike and inverse effect of SMF on the PSI. An increment of PSI emission was evident for SMF treated dark control thylakoid membrane fractions (normal pH) whereas bio-energetically perturbed membrane fractions inverted the effect upon SMF exposure. At a bio-energetically destabilized condition SMF behaved reversibly (flip-flop). Whereas the same bio-energetically destabilized membrane fractions at no field conditions mimicked the PSI enhancement. (Fig. 8). SMF, low pH and effector influence on the membrane fractions were summarized in Table 2.

The fluorescence emission of P_{723}/P_{689} was found to be susceptible to the membrane diffusional properties, structural alterations and packing of complexes in the photosynthetic membranes. Thylakoid membrane

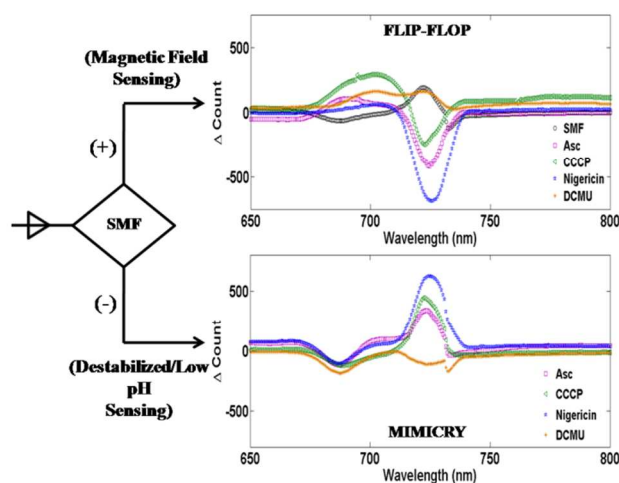


Fig. 8. Reversible and mimicking effects of SMF on photon capture circuit of the photosynthetic machinery. The figure represents the difference spectral images of normal pH and effector treated membranes with concomitant SMF exposure (flip-flop) and only effector treated membranes with no SMF perturbation (mimicry). Top image represents effector subtracted from SMF and SMF at normal pH (black circle) and the bottom image represents effector subtracted from dark control values at no field condition.

Table 2. The fractional distribution of the photosynthetic membrane (PSI and PSII) with respect to (effectors and SMF and both) perturbation. $\Delta \ln \text{PS(I or II)} = [\Delta \text{PS(I or II)}] / [\text{PS(I or II)}]$; $\Delta = (\text{final} - \text{initial})$. The PSI/PSII ratio for the control is 1.

SAMPLE	PSI/PSII	$\Delta \ln \text{PSI}$	$\Delta \ln \text{PSII}$	$(\Delta \ln \text{PSI} / \Delta \ln \text{PSII})$
Control +SMF	1.732	0.603	0.021	30.15
Relaxation	1.482	0.182	0.087	2.09
Nigericin Effect	2.853	2.01	0.1769	11.36
Nigericin + SMF	1.195	0.383	0.287	1.334
L-Asc Effect	2.148	0.408	0.186	2.19
L-Asc + SMF	1.04	-0.058	0.0248	-2.33
CCCP	2.633	1.471	0.0068	216.3
CCCP + SMF	1.272	0.96	0.652	1.472
DCMU	1.469	-0.11	-0.301	0.365
DCMU + SMF	1.394	0.155	0.044	-3.522

components (grana appressed and stroma margins) were previously reported to exhibit dynamic lateral diffusion

and swelling upon generation of ΔpH^{54} and light. In the present context, thylakoids exert spin modulated morphological and diffusional alteration of the membrane surface topography upon SMF perturbation. The SMF induced spin dependent structural alterations such as membrane re-organization and re-assembly with a distinct change of intra-membrane alignment after SMF exposure were revealed from the AFM images represented in Fig. 9 (a, b).

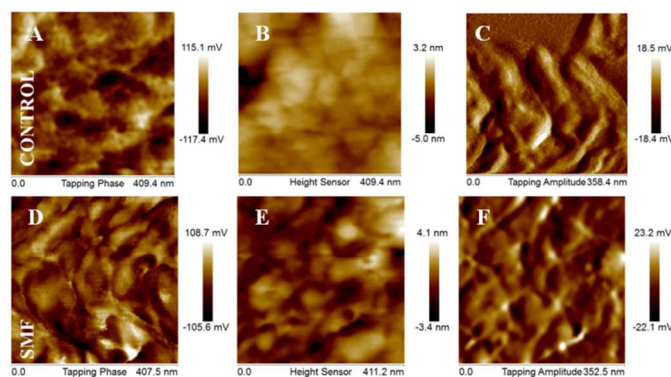


Fig. 9(a). Surface topographical profiling of the thylakoid membrane fractions upon SMF treatment. The phase, height and amplitude profile of the dark adapted thylakoid membrane fractions (A-C) and the SMF treated membrane fractions (D-F) showing spin dependent structural realignment. Scale bar for figure A, B, D, E is ~ 410 nm and ~ 350 nm for figure C and F (amplitude profile). The electrical measurement of the tapping phase and amplitude profile were represented in mV while the mechanical height profile (vertical and horizontal) were imaged at nano-meter (nm) scale.

The amplitude profile of the native thylakoid membranes are consistent with the continuous helical model of the thylakoids⁵⁵ denoting connectivity of some stroma lamellae to the top of the granum while adjunction of some at the bottom. The surface properties of the dark adapted thylakoid membranes decipher

flattened sac like membranous invaginations measured to be of $\sim 300 \pm 100$ nm grana dimensions consistent with previous literature reports. The topographical profile of the dark adapted thylakoid membrane fractions (Fig. 9a, A-C) clearly indicate SMF induced bulk scale topographical re-arrangement (Figure. 9a, D-F). SMF perturbation lead to spin modulated repressing and re-alignment (phase profile) of the membrane components with distinct orientation revealing $\sim 200 \pm 50$ nm membrane protrusions accompanied with elevated tuft and twigs in the vertical depth deciphered from the height images. The spin dependent re-modelling effect was thus translated to exert an increased size and compactness of the membrane surface components with respect to the un-treated ones (Fig. 9b).

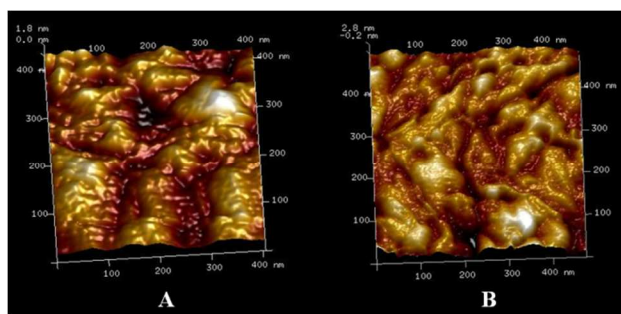


Fig.9(b). Three dimensional projection of the height profile of the thylakoid membrane fractions before (A) and after SMF (B) perturbation. The vertical distance difference were 1.8 nm and 2.6 nm for control and SMF treated membranes respectively. Scale bar for the images were 400 nm.

Whereas, the protonophore treated dark adapted thylakoid membrane fractions indicate PSI specific membrane topographic signature consistent with the targeted action of protonophore to PSI. Protonophore action dissipates the proteic kinetic barrier and effects the easily accessible un-appressed and Δp regulating PSI

bearing stroma membranes. Ring like surface protrusions of 40 ± 10 nm were observed in both the nigericin and CCCP treated membranes. This specialized structures may be indicative of the protonophore susceptible stromal complex.

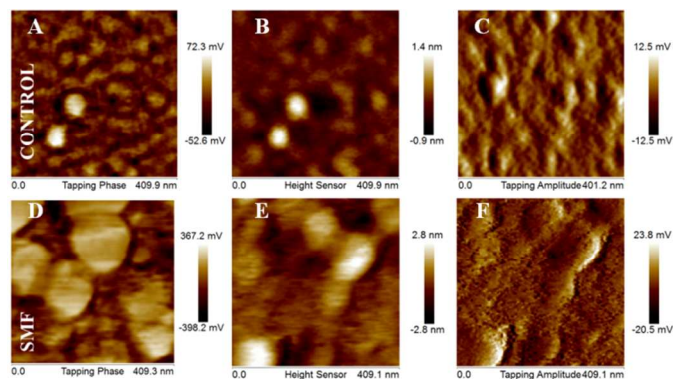


Fig. 10. Dynamic surface distribution properties of the nigericin treated dark adapted thylakoid membrane fractions upon SMF treatment. The phase, height and amplitude profile of the thylakoid membrane fractions (A-C) and the SMF treated membranes (D-F) exhibiting spin dependent structural re-assembly. Scale bar for figures are ~ 400 -410 nm.

The rings were found to disappear upon SMF treatment to re-form distinct spherical appressed regions indicative of granum, interconnected to non-appressed and flattened surface of stroma lamellae and margins (Fig. 10, 11).

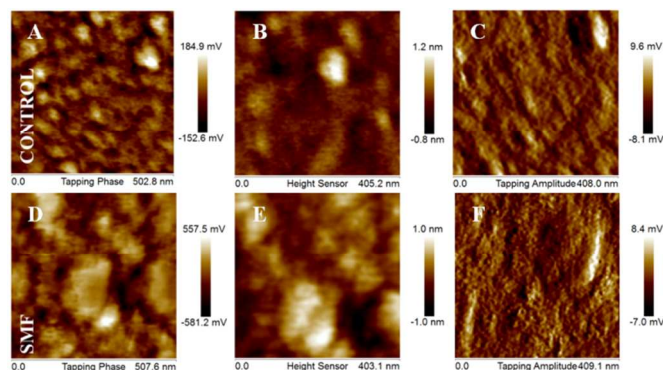


Fig. 11. Surface properties of the CCCP treated thylakoid membranes upon SMF treatment. The phase, height and amplitude profile of the dark adapted thylakoid membrane fractions (A-C) and the SMF treated fractions (D-F) were indicative of spin dependent membrane re-distribution. Scale bar for figure A and D is ~ 500nm and ~400 nm for figure B,C,E and F.

Re-assembly of the membrane lamellar components with an increase in size and reformation of 150 ± 50 nm tubular structures were evident from the surface images. Thus a spin controllable efficient synthetic control over photosynthetic circuit is thus possible utilizing this system.

Discussions

In a structure like thylakoid membrane with high degree of organizational complexity and localization of magnetic centres (Mn clusters, Fe-S centres) and intrinsic dipole transition moment of chlorophylls, accessory pigment and protein molecules, generation of an effective magnetic moment component in response to any externally applied SMF is plausible, due to the conservation of magnetic moment.

At normal pH, SMF exposure mimicked the bio-energetically destabilized state of the membrane as both Δp collapse (by nigericin, CCCP and L-Asc) and exposure to SMF caused PSI(P_{723}) to increase. At a bio-energetically uncoupled state this increment is reversible with SMF. Thus, we can modify the general equation of electrochemical proton gradient generated across the bi-layer membrane⁵⁶,

$$\Delta p = \Delta \Psi - (RT/F) \Delta pH \dots(2)$$

to,

$$\Delta p = - (RT/F) \Delta pH - \mu.H/F \dots(3)$$

where, H denotes the externally applied field strength (SMF), μ denotes the magnetic moment component of the bio-energetic status of the membrane fractions, F being the Faraday constant.

The generation of an additional magnetic moment μ can be mediated through a coherent spin assembly, the SMF being a spin perturbation. A component of such magnetic moment may also be contributed by the ferromagnetic Mn/Fe centres of the photo-system or by altered cyclic electron or proton flow. It may be further noted that the sign of $-\mu.H/F$, may be sensitive to the external pH, as the magnetic moment generation depends on the spin carrying ligands and the local molecular environment of the ferromagnetic centres.

At dark adapted state any proteic perturbation or exposure to SMF may generate this additional negative proton motive contribution yielding a reversible uncoupling like effect. This simple model can explain the SMF induced reduction of PSI/PSII ratio, if we postulate that at low pH or in presence of protonophores a positive contribution of $-\mu.H/F$ restores the membrane to its normal resting phase. However the effect of such small perturbation can be amplified by the proton flow associated with such perturbation (Scheme 1).

It is this transient proton flux that makes the SMF mimic the uncouplers and it is this effect that ultimately reflects in the optical transition that we have reported.

The overall enhancement of photon capture efficiency is a positive effect and this effect unlike uncouplers is performed without true uncoupling, as the relaxation patterns shows the process is truly reversible. The reverse optical transition seen at lower pH also suggests that the SMF interacts with the coherent milieu of the thylakoid by targeting the proteic flow and the other effects like bulk changes in diffusional behaviour may

be an associated secondary consequence of this proteic target.

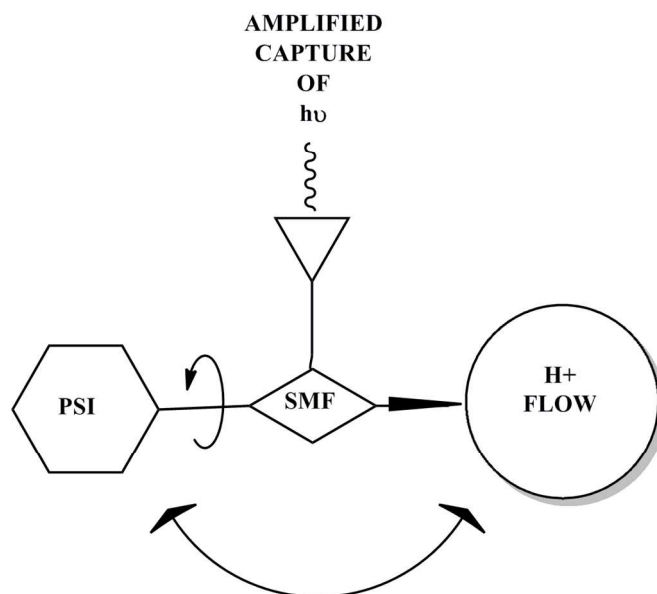
It may be noted that the usual arguments in favour of fluorescence enhancement as reported¹¹ will not be valid here as the experimental conditions involved pre-exposition rather than real time exposition of SMF. We report effects at post magnetic incubation stage where radical pair mechanism demands instantaneous Zeeman splitting. The magnetic perturbation in energy terms is much less than the thermal energy (kT). The amplification of such minor spins perturbation cannot be explained by diamagnetic susceptibility as much higher magnetic strength (typically of the order of 5-10T) may be needed for any observable diamagnetic change. Secondly diamagnetic properties would have shown no slow relaxation behaviour. However spin relaxation seems to be a feasible option for such slow relaxation and this may be manifested in a coherent system like thylakoid.

Conclusions

The paper shows that perturbed proton flow may be a primary target of the SMF which may be amplified through secondary proton or electron coupled processes. The explanation is in agreement with quantum description that postulates a spatiotemporal coherence in the thylakoid membranes. In contrary, one cannot classically explain why the SMF induced spin perturbation is not masked by the thermal energy as $kT \gg \mu.H$. The quantum perturbation is sensed by the proteic circuit which can serve as a mediator for inter-photo-system energy transition and other bulk phase long term (or large scale) changes.

The other important issues raised in this paper are, one can obtain an uncoupling like action by SMF, SMF can

reverse the protonophore action and SMF can artificially enhance the photon capture efficiency, effects having important practical implications.



Scheme 1. SMF induced amplification of photon capture. PSI driven proton flow (coupled cyclic electron flow controlling Δp) as a target for spin perturbation. SMF effect was amplified by proton flow at normal (cyclic arrow) and effector destabilized conditions (elongated thick arrow) through PSI.

Acknowledgements

We gratefully thank Department of Biotechnology, Govt. of India (09/71AGOI) IPLS for supporting the research. We cordially thank Dr. Alok Sil and Ms. Puja Biswas for providing excellent assistance in acquiring the AFM images.

Notes and references

Department of Biochemistry; University of Calcutta; 35, Ballygunge Circular Road; Kolkata-700019; India.

Fax: +9133-24614849; Telephone: +919748758663

adbic@caluniv.ac.in adgcal@gmail.com;

†These authors contributed equally in this work.

†Electronic Supplementary Information (ESI) available: [Supporting information has been provided online].

See DOI: 10.1039/b000000x/

1. N. Belyavskaya, Biological effects due to weak magnetic field on plants, *Advances in Space Research*, 2004, **34**, 1566-1574.
2. A. Hoff, Magnetic field effects on photosynthetic reactions, *Q. Rev. Biophys.*, 1981, **14**, 599.
3. H. Lee, Y.-C. Cheng and G. R. Fleming, Coherence dynamics in photosynthesis: protein protection of excitonic coherence, *Science*, 2007, **316**, 1462-1465.
4. J. M. Olson, The FMO Protein, *Photosynthesis research*, 2004, **80**, 181-187.
5. G. Panitchayangkoon, D. Hayes, K. A. Fransted, J. R. Caram, E. Harel, J. Wen, R. E. Blankenship and G. S. Engel, Long-lived quantum coherence in photosynthetic complexes at physiological temperature, *Proceedings of the National Academy of Sciences*, 2010, **107**, 12766-12770.
6. D. P. Small, N. Hüner and W. Wan, Effect of static magnetic fields on the growth, photosynthesis and ultrastructure of *Chlorella kessleri* microalgae, *Bioelectromagnetics*, 2012, **33**, 298-308.
7. S. Pietruszewski, S. Muszynski and A. Dziwulska, Electromagnetic fields and electromagnetic radiation as non-invasive external stimulants for seeds (selected methods and responses), *International agrophysics*, 2007, **21**, 95.
8. P. Galland and A. Pazur, Magnetoreception in plants, *Journal of plant research*, 2005, **118**, 371-389.
9. T. Ritz, T. Yoshii, C. Foerster and M. Ahmad, Cryptochrome: A photoreceptor with the properties of a magnetoreceptor?, *Communicative & integrative biology*, 2010, **3**, 24-27.
10. T. Yoshii, M. Ahmad and C. Helfrich-Förster, Cryptochrome mediates light-dependent magnetosensitivity of *Drosophila*'s circadian clock, *PLoS biology*, 2009, **7**, e1000086.
11. J. R. Norris, TRIPLET STATES AND PHOTOSYNTHESIS, *Photochemistry and Photobiology*, 1976, **23**, 449-450.
12. A. Ishizaki and G. R. Fleming, Quantum coherence in photosynthetic light harvesting, *Annu. Rev. Condens. Matter Phys.*, 2012, **3**, 333-361.
13. I. Kassal, J. Yuen-Zhou and S. Rahimi-Keshari, Does coherence enhance transport in photosynthesis?, *The Journal of Physical Chemistry Letters*, 2013, **4**, 362-367.
14. M. Tikkanen, M. Nurmi, M. Suorsa, R. Danielsson, F. Mamedov, S. Styring and E.-M. Aro, Phosphorylation-dependent regulation of excitation energy distribution between the two photosystems in higher plants, *Biochimica et Biophysica Acta (BBA)-Bioenergetics*, 2008, **1777**, 425-432.
15. J. P. Dekker and E. J. Boekema, Supramolecular organization of thylakoid membrane proteins in green plants, *Biochimica et Biophysica Acta (BBA)-Bioenergetics*, 2005, **1706**, 12-39.
16. E. Shimoni, O. Rav-Hon, V. Brumfeld and Z. Reich, Three-dimensional organization of higher-plant chloroplast thylakoid membranes revealed by electron tomography, *The Plant Cell Online*, 2005, **17**, 2580-2586.
17. N. Nelson and A. Ben-Shem, The complex architecture of oxygenic photosynthesis, *Nature Reviews Molecular Cell Biology*, 2004, **5**, 971-982.
18. Y. Evron and R. E. McCarty, Simultaneous measurement of ΔpH and electron transport in chloroplast thylakoids by 9-aminoacridine fluorescence, *Plant physiology*, 2000, **124**, 407-414.
19. S. Saphon and A. R. Crofts, The H⁺/e⁻-ratio in chloroplasts is 2. Possible errors in its determination, *Z Naturforsch 32c*, 1977, 810-816.
20. T. Owens, S. Webb, L. Mets, R. Alberte and G. Fleming, Antenna size dependence of fluorescence decay in the core antenna of photosystem I: estimates of charge separation and energy transfer rates, *Proceedings of the National Academy of Sciences*, 1987, **84**, 1532-1536.
21. U. Schreiber, W. Bilger and C. Neubauer, Chlorophyll fluorescence as a noninvasive indicator for rapid assessment of in vivo photosynthesis, in *Ecophysiology of photosynthesis*, Springer, 1994, pp. 49-70.
22. D. M. Kramer, J. A. Cruz and A. Kanazawa, Balancing the central roles of the thylakoid proton gradient, *Trends in plant science*, 2003, **8**, 27-32.
23. K. Takizawa, J. A. Cruz, A. Kanazawa and D. M. Kramer, The thylakoid proton motive force Δp in vivo. Quantitative, non-invasive probes, energetics, and regulatory consequences of light-induced Δp , *Biochimica et Biophysica Acta (BBA)-Bioenergetics*, 2007, **1767**, 1233-1244.
24. S. Theg, G. Chiang and R. Dilley, Protons in the thylakoid membrane-sequestered domains can directly pass through the coupling factor during ATP synthesis in flashing light, *Journal of Biological Chemistry*, 1988, **263**, 673-681.
25. H. Yamasaki, S. Furuya, A. Kawamura, A. Ito, S. Okayama and M. Nishimura, Induction of the H⁺ release from thylakoid membranes by illumination in the presence of protonophores at high concentrations, *Plant and cell physiology*, 1991, **32**, 925-934.
26. M. Huber, Introduction to magnetic resonance methods in photosynthesis, *Photosynthesis research*, 2009, **102**, 305-310.
27. C. R. Timmel and K. B. Henbest, A study of spin chemistry in weak magnetic fields, *Philosophical Transactions of the Royal Society of London. Series A: Mathematical, Physical and Engineering Sciences*, 2004, **362**, 2573-2589.
28. N. Bukhov and R. Carpentier, Alternative photosystem I-driven electron transport routes: mechanisms and functions, *Photosynthesis research*, 2004, **82**, 17-33.
29. Y. Munkage and T. Shikanai, Cyclic electron transport through photosystem I, *Plant biotechnology*, 2005, **22**, 361-369.
30. H. Takahashi, S. Clowez, F.-A. Wollman, O. Vallon and F. Rappaport, Cyclic electron flow is redox-controlled but independent of state transition, *Nature communications*, 2013, **4**.
31. S. Santabarbara, I. Kuprov, W. V. Fairclough, S. Purton, P. J. Hore, P. Heathcote and M. C. Evans, Bidirectional electron transfer in photosystem I: determination of two distances between P700⁺ and A1-in spin-correlated radical pairs, *Biochemistry*, 2005, **44**, 2119-2128.
32. Y.-S. Jung, I. R. Vassiliev and J. H. Golbeck, Crossover of a high-spin ($S = 7/2, 3/2$) to a low-spin ($S = 1/2$) iron-selenium cluster in FA and FB of photosystem I on rebinding of PsaC onto P700-FX cores, *JBIC Journal of Biological Inorganic Chemistry*, 1997, **2**, 209-217.
33. K. A. Campbell, W. Gregor, D. P. Pham, J. M. Peloquin, R. J. Debus and R. D. Britt, The 23 and 17 kDa extrinsic proteins of photosystem II modulate the magnetic properties of the S1-state manganese cluster, *Biochemistry*, 1998, **37**, 5039-5045.
34. R. Inglis, C. C. Stoumpos, A. Prescimone, M. Siczek, T. Lis, W. Wernsdorfer, E. K. Brechin and C. J. Milios, Ferromagnetic manganese "cubes": from PSII to single-molecule magnets, *Dalton transactions (Cambridge, England : 2003)*, 2010, **39**, 4777-4785.
35. Y. Kurashige, G. K.-L. Chan and T. Yanai, Entangled quantum electronic wavefunctions of the Mn₄CaO₅ cluster in photosystem II, *Nature Chemistry*, 2013.
36. U. Heinen, O. Poluektov, E. Stavitski, T. Berthold, E. Ohmes, S. L. Schlesselman, J. R. Golecki, G. J. Moro, H. Levanon and M. C. Thurnauer, Magnetic-field-induced orientation of photosynthetic reaction centers, as revealed by time-resolved D-band electron paramagnetic resonance of spin-correlated radical pairs. II. Field dependence of the alignment, *The Journal of Physical Chemistry B*, 2004, **108**, 9498-9504.
37. Z. Zeng, D. Guenzburger and D. Ellis, Electronic structure, spin couplings, and hyperfine properties of nanoscale molecular magnets, *Physical Review B*, 1999, **59**, 6927.
38. B. Brocklehurst, Magnetic fields and radical reactions: recent developments and their role in nature, *Chemical Society Reviews*, 2002, **31**, 301-311.
39. G. Scott, Review of gyromagnetic ratio experiments, *Reviews of Modern Physics*, 1962, **34**, 102.
40. D. J. Müller and Y. F. Dufréne, Atomic force microscopy: a nanoscopic window on the cell surface, *Trends in cell biology*, 2011, **21**, 461-469.
41. D. J. Muller, AFM: A Nanotool in Membrane Biology, *Biochemistry*, 2008, **47**, 7986-7998.
42. R. Garcia and R. Perez, Dynamic atomic force microscopy methods, *Surface science reports*, 2002, **47**, 197-301.
43. H. Kirchhoff, Molecular crowding and order in photosynthetic membranes, *Trends in plant science*, 2008, **13**, 201-207.

44. M. Herbstová, S. Tietz, C. Kinzel, M. V. Turkina and H. Kirchhoff, Architectural switch in plant photosynthetic membranes induced by light stress, *Proceedings of the National Academy of Sciences*, 2012, **109**, 20130-20135.
45. D. Kaftan, V. Brumfeld, R. Nevo, A. Scherz and Z. Reich, From chloroplasts to photosystems: in situ scanning force microscopy on intact thylakoid membranes, *The EMBO journal*, 2002, **21**, 6146-6153.
46. S. G. Chuartzman, R. Nevo, E. Shimoni, D. Charuvi, V. Kiss, I. Ohad, V. Brumfeld and Z. Reich, Thylakoid membrane remodeling during state transitions in Arabidopsis, *The Plant Cell Online*, 2008, **20**, 1029-1039.
47. A. Hazra and M. DasGupta, Phosphorylation-dephosphorylation of light-harvesting complex II as a response to variation in irradiance is thiol sensitive and thylakoid sufficient: modulation of the sensitivity of the phenomenon by a peripheral component, *Biochemistry*, 2003, **42**, 14868-14876.
48. J. Bennett, K. E. Steinback and C. J. Arntzen, Chloroplast phosphoproteins: regulation of excitation energy transfer by phosphorylation of thylakoid membrane polypeptides, *Proc Natl Acad Sci U S A*, 1980, **77**, 5253-5257.
49. M. Hipkins and N. R. Baker, *Photosynthesis: energy transduction: a practical approach*, IRL Press Limited, 1986.
50. C. Sigalat, Y. de Kouchkovsky and F. Haraux, Flow-force relationships in lettuce thylakoids. 2. Effect of the uncoupler FCCP on local proton resistances at the ATPase level, *Biochemistry*, 1993, **32**, 10201-10208.
51. J. N. Sturgis, J. D. Tucker, J. D. Olsen, C. N. Hunter and R. A. Niederman, Atomic Force Microscopy Studies of Native Photosynthetic Membranes†, *Biochemistry*, 2009, **48**, 3679-3698.
52. P. Manna and W. Vermaas, Lumenal proteins involved in respiratory electron transport in the cyanobacterium *Synechocystis* sp. PCC6803, *Plant molecular biology*, 1997, **35**, 407-416.
53. G. Forti and A. M. Ehrenheim, The role of ascorbic acid in photosynthetic electron transport, *Biochimica et Biophysica Acta (BBA)-Bioenergetics*, 1993, **1183**, 408-412.
54. G. Cornic, N. G. Bukhov, C. Wiese, R. Blligny and U. Heber, Flexible coupling between light-dependent electron and vectorial proton transport in illuminated leaves of C3 plants. Role of photosystem I-dependent proton pumping, *Planta*, 2000, **210**, 468-477.
55. L. Mustárdy, Development of thylakoid membrane stacking, in *Oxygenic photosynthesis: the light reactions*, Springer, 1996, pp. 59-68.
56. P. Mitchell, *Chemiosmotic coupling in energy transduction: a logical development of biochemical knowledge*, Springer, 1974.